# In Situ Monitoring of Kinetics of Charged Thiol Adsorption on Gold Using an Atomic Force Microscope

Kai Hu and Allen J. Bard*

*Department of Chemistry and Biochemistry, The University of Texas at Austin, Austin, Texas 78712*

*Received December 12, 1997. In Final Form: June 12, 1998*

The adsorption of a charged thiol ($HSC_{10}COO^-$) on gold from its aqueous solutions of different concentration was monitored in situ by probing the surface charge. This was accomplished by measuring the interfacial forces between a modified (with a negatively charged silica sphere) tip of an atomic force microscope and the thiol-adsorbed gold surface as a function of adsorption time. The surface charge and potential were then deduced from the force data. If a Langmuir rate law is employed to fit the overall surface coverage vs time data, average observed adsorption rate constants of 0.045 ± 0.005 (0.5 mM) and 0.020 ± 0.003 (0.05 mM) $min^{-1}$ were obtained and were dependent on thiol concentration. The self-assembly process was a two-step process, an initial fast step followed by a slow step.

## Introduction

Self-assembled monolayers (SAMs) are molecular assemblies formed by spontaneous adsorption of thiolates on gold.[1−3] This irreversible adsorption process offers well-organized molecular structures which allow for surface modification. Assemblies of this type provide a convenient and rational approach for controlling the surface chemical and physical properties such as wettability, adhesion, adsorption, charge state, etching behavior, and chemical reactivity.[4−11] A variety of experimental techniques have been applied in studies of these SAMs to elucidate their molecular-scale structural properties. From such studies, some aspects of the molecular self-assembly behavior are clear. For example, the self-assembly process is energetically favorable due to the gold thiolate bond formation and the hydrophobic attraction between aliphatic chains. The resulting monolayer is composed of densely packed, virtually all-trans aliphatic chains that are tilted at ~30° with respect to the surface normal.

Most SAM studies to date have focused on investigating the fully covered substrates and their various applications. There have been relatively few studies of the adsorption kinetics of the SAM formation process. Bain et al.[4] studied the formation process of octadecanethiol layers on gold from ethanol solutions. The adsorption kinetics were monitored ex situ by measuring the thickness via ellipsometry and the wettability of the layer by contact-angle measurements. More recently, several research groups investigated the rate of alkanethiol SAM formation by in situ or ex situ quartz crystal microbalance (QCM) techniques.[12−15] Peterlinz and Georgiadas also studied SAM formation kinetics by surface plasmon resonance spectroscopy.[16] However, the results of the previous studies on this subject are not entirely consistent; i.e., there are substantial differences among the reported time scales for the adsorption process, ranging from seconds to 10−20 h. As pointed out in a recent report by Pan et al.,[15] there are several important factors that can be responsible for these considerable differences in the reported kinetics of alkanethiol adsorption onto gold, e.g., the presence of preadsorbed contaminants on the Au, the solution-phase mass-transfer processes, the difference between in situ and ex situ methods, and solvent effects. In this report, the adsorption rate of a charged thiol on gold from aqueous solution was monitored in situ by probing the surface charge. This was accomplished by measuring the interfacial forces between a charged tip of an atomic force microscope (AFM) and the gold surface at different stages of the SAM formation.

Recent advances in force measurements associated with the AFM have allowed direct force measurements between a sphere and a flat surface.[17−19] These direct measurements of surface forces have significantly advanced our understanding of interfacial processes.[20] In an AFM force measurement, the deflection of a microfabricated cantilever is measured as a function of its separation from a surface. In a previous study,[11] we demonstrated that the

---

(1) Nuzzo, R. G.; Allara, D. J. *J. Am. Chem. Soc.* **1983**, *105*, 4481.
(2) Allara, D. J.; Nuzzo, R. G. *Langmuir* **1985**, *1*, 45.
(3) Ulman, A. *An Introduction to Ultrathin Organic Films: From Langmuir*−*Blodgett to Self-Assembly*; Academic Press: Boston, 1991.
(4) Bain, C. D.; Troughton, E. B.; Tao, Y.-T.; Evall, J.; Whitesides, G. M.; Nuzzo, R. G. *J. Am. Chem. Soc.* **1989**, *111*, 321.
(5) Bain, C. D.; Whitesides, G. M. *Angew. Chem., Int. Ed. Engl.* **1989**, *28*, 506.
(6) Dubois, L. H.; Nuzzo, R. G. *Annu. Rev. Phy. Chem.* **1992**, *43*, 437.
(7) Mirkin, C. A.; Ratner, M. A. *Annu. Rev. Phy. Chem.* **1992**, *43*, 719.
(8) Kim, E.; Kumar, A.; Whitesides, G. M. *J. Electrochem. Soc.* **1995**, *142*, 628.
(9) Yamamoto, Y.; Nishihara, H.; Aramaki, K. *J. Electrochem. Soc.* **1993**, *140*, 436.
(10) Laibinis, P. E.; Whitesides, G. M. *J. Am. Chem. Soc.* **1992**, *114*, 9022.
(11) Hu, K.; Bard, A. J. *Langmuir* **1997**, *13*, 5114.
(12) Shimazu, K.; Yag, I.; Sato, Y.; Uosaki, K. *Langmuir* **1992**, *8*, 1385.
(13) Kim, Y. T.; McCarley, R. L.; Bard, A. J. *Langmuir* **1993**, *9*, 1941.
(14) Karpovich, D. S.; Blanchard, G. J. *Langmuir* **1994**, *10*, 3315.
(15) Pan, W.; Durning, C. J.; Turro, N. J. *Langmuir* **1996**, *12*, 4469.
(16) Peterlinz, K. A.; Georgiadis, R. *Langmuir* **1996**, *12*, 4731.
(17) (a) Ducker, W. A.; Senden, T. J.; Pashley, R. M. *Nature* **1991**, *353*, 239. (b) Ducker, W. A.; Senden, T. J.; Pashley, R. M. *Langmuir* **1992**, *8*, 1831.
(18) (a) Biggs, S.; Mulvaney, P.; Zukoski, C. F.; Grieser, F. *J. Am. Chem. Soc.* **1994**, *116*, 9150. (b) Larson, I.; Drummond, C. J.; Chan, D. Y. C.; Grieser, F. *J. Am. Chem. Soc.* **1993**, *115*, 11885. (c) Li, Y. Q.; Tao, N. J.; Pan, J.; Garcia, A. A.; Lindsay, S. M. *Langmuir* **1993**, *9*, 637. (d) Atkins, D. T.; Pashley, R. M. *Langmuir* **1993**, *9*, 2232. (e) Larson, I.; Drummond, C. J.; Chan, D. Y. C.; Grieser, F. *J. Phys. Chem.* **1995**, *99*, 2114.
(19) Hillier, A. C.; Kim, S.; Bard, A. J. *J. Phys. Chem.* **1996**, *100*, 18808.
(20) (a) Derjaguin, B. V.; Rabinovich, Y. I.; Churaev, N. V. *Nature* **1978**, *272*, 313. (b) Israelachvili, J. N. *Intermolecular and Surface Forces*, 2nd ed.; Academic Press: New York, 1991.

S0743-7463(97)01363-2 CCC: $15.00

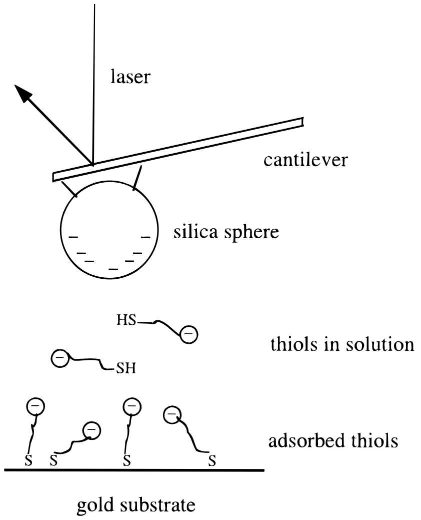

**Figure 1.** Schematic representation of the AFM force measurement between a negatively charged silica sphere and a thiol-covered gold substrate in 0.5 mM $HSC_{10}COO^-$ aqueous solution at pH 10.2.

AFM could be used to measure the pH-dependent double-layer forces at a carboxylic acid-terminated SAM surface. Here we extend this work and apply the same methodology to monitor in situ the adsorption process of a charged thiol, fully deprotonated mercaptoundecanoic acid ($HSC_{10}COO^-$), on gold from its aqueous solution as a function of adsorption time. More specifically, the diffuse double layer at the charged thiol adsorbed gold surface is probed with nanonewton force resolution with a modified silica spherical tip on the cantilever of an AFM (Figure 1). The surface charge and potential are then calculated from the force data. From the surface coverage vs time data, kinetic information about the SAM formation is obtained. To our knowledge, this is the first demonstration of AFM force measurement to study quantitatively the kinetics of thiol adsorption on gold.

## Experimental Section

**Materials.** The SAM species, mercaptoundecanoic acid ($HSC_{10}COOH$), was kindly supplied by Professor Richard Crooks (Texas A&M University). The aqueous solutions of mercaptoundecanoic acid (0.5 and 0.05 mM) were freshly prepared with 18 MΩ deionized water (Milli-Q Plus, Millipore Corp., Bedford, MA). The solution was adjusted to pH 10.2 with 0.01 M NaOH to obtain fully deprotonated, negatively charged thiols in solution. The solution of 0.5 mM NaCl at pH 10.2 was prepared in a similar way. Immediately before use, all solutions were deaerated with argon for 20 min.

Commercial glass cover slips cut into 1 $cm^2$ squares were used as silica substrates. Prior to use, the silica substrates were cleaned in a concentrated sulfuric/nitric acid (1:1) solution, followed by exposure to condensing steam vapor for 30 min. Large, flat, template-stripped gold surfaces with (111) orientation were prepared according to the method of Hegner et al.[21] In the control experiments for measuring the surface charge of fully covered SAM/Au substrates, the freshly prepared template-stripped gold surface was immediately immersed into a 5 mM mercaptoundecanoic acid ethanolic solution for 24 h. Immediately prior to use, the SAM-covered gold substrate was rinsed with EtOH for 30 s and dried under argon. The microfabricated AFM cantilever was modified by attaching a silica sphere in a fashion similar to the procedure of Ducker et al.[17b] Before each experiment, the force-sensing silica tip was rinsed with EtOH, rinsed with purified water, and blown dry with argon.

**Force Measurements.** Force measurements were performed with a Nanoscope III AFM (Digital Instruments, Santa Barbara, CA) equipped with a piezo scanner having a maximum scan range of 15 $\mu$m × 15 $\mu$m × 2 $\mu$m. The AFM force measuring technique is well-documented.[17−19] Typically, in an AFM force measurement, the deflection of a microfabricated cantilever is measured as a function of its separation from a surface. The spring constant of the modified cantilever was determined using the method of Cleveland et al.[22] and was found to be 0.65 ± 0.12 N/m.

**AFM Data Analysis.** During the force measurement, the measured experimental parameters were the cantilever deflection, obtained from the voltage of the sectored photodiode detector, and the substrate displacement, which was given by the piezo scanner voltages. These data were converted to a normalized force (force/radius) vs tip−substrate separation for further analysis. Derjaguin−Landau−Verwey−Overbeek (DLVO) theory[23] was employed to calculate the surface electrostatic potentials between the similarly charged surfaces, i.e., the interaction between two silica surfaces. The electrical double-layer interaction energy between dissimilarly charged surfaces, such as the silica−gold interaction, was calculated for the constant-potential and constant-charge limits of the complete nonlinear Poisson−Boltzmann equation using the method of Hillier et al.[19] The Hamaker constants ($A_H$) for the silica−silica and silica−gold interactions were $0.88 \times 10^{-20}$ J[24] and $1.1 \times 10^{-19}$ J,[11,19] respectively.

**Procedure.** In a typical experiment, the silica sphere (10−20 $\mu$M diameter) was mounted into a precleaned AFM liquid cell (Digital Instruments), while the substrate was a freshly prepared template-stripped gold surface. The solution of 0.5 mM mercaptoundecanoic acid (pH 10.2) was injected into the liquid cell, and the force−distance data were then collected as a function of time. In order to not perturb the SAM formation process, the silica probe was engaged only at the moment when the force curves were collected. For those force curves obtained within 2 min, the procedure was as follows. The solution of 0.5 mM NaCl (pH 10.2) was first injected into the liquid cell, and the silica probe was then engaged. The solution of NaCl was replaced by the solution of 0.5 mM mercaptoundecanoic acid (pH 10.2) while the silica tip was still in operation. In this way, the double-layer force could be monitored continuously at the initial stages of the SAM formation.

## Results and Discussion

**Calibration of Silica Probe.** Force measurements between a silica sphere and a silica substrate were conducted to determine the silica surface potential under conditions similar to those used while probing the double layers at the thiol-adsorbed gold substrates. Solutions of 0.5 mM NaCl and 0.5 mM mercaptoundecanoic acid at pH 10.2, were examined. The silica surfaces are negatively charged at a solution pH of 10.2 and diffuse double layers form at the interfaces. AFM force measurements can probe the double-layer structure and thickness as the tip penetrates the double layer. Generally, these force−distance curves exhibited an exponential dependence with distance that was well reproduced by standard DLVO theory.[23] The measured silica surface potential was −55 mV under these conditions. The Debye length, $\kappa^{-1}$, of the diffuse double layer was 11.5 nm, in good agreement with that calculated from the salt concentration of the solutions.[25] The force curves collected in 0.5 mM NaCl and

---

[21] Hegner, M.; Wagner, P.; Semenza, G. *Surf. Sci.* **1993**, 291, 39.

[22] (a) Cleveland, J. P.; Manne, S.; Bocek, D.; Hansma, P. K. *Rev. Sci. Instrum.* **1993**, *64*, 403. (b) Sader, J. E.; Larson, I.; Mulvaney, P.; White, L. R. *Rev. Sci. Instrum.* **1995**, *66*, 3789.

[23] (a) Derjaguin, B. V. *Trans. Faraday Soc.* **1940**, *36*, 203. (b) Derjaguin, B. V.; Landau, L. D. *Acta Physica Chem.* **1941**, *14*, 633. (c) Derjaguin, B. V.; Landau, L. D. *J. Exp. Theor. Phys.* **1941**, *11*, 802. (d) Verwey, E. J. W.; Overbeek, J. T. G. *Theory of the Stability of Lyophobic Colloids*; Elsevier: New York, 1948.

[24] (a) Grabbe, A.; Horn, R. G. *J. Colloid Interface Sci.* **1993**, *157*, 375. (b) Hunter, R. J. *Foundations of Colloid Science*; Oxford University Press: Oxford, 1987. (c) Hough, D. B.; White, L. R. *Adv. Colloid Interface Sci.* **1980**, *81*, 285.

[25] For dilute aqueous solutions containing 1:1 electrolyte at 25 °C, the Debye length is given by $\kappa^{-1} = 0.3045/C^{1/2}$, where $C$ is the ion concentration of the $z$:$z$ electrolyte.

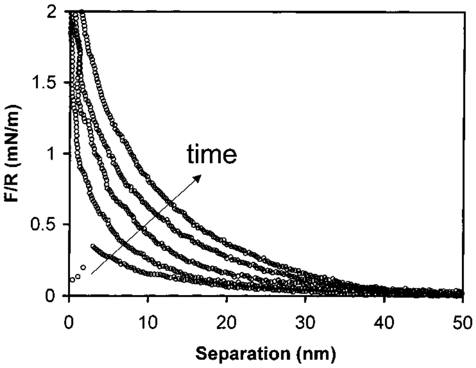

**Figure 2.** Force between a silica probe and thiol-adsorbed gold substrate in a 0.5 mM $HSC_{10}COO^-$ aqueous solution at pH 10.2 as a function of adsorption time. The force is scaled to the probe radius ($R = 8.0$ $\mu$m). The force curves correspond to adsorption times, from bottom to top, of 0.33, 2.5, 10, 30, and 180 min.

0.5 mM mercaptoundecanoic acid aqueous solutions of pH 10.2 were exactly the same, indicating that the ionic nature of the charged thiol is the same as that of NaCl, a completely dissociated simple 1:1 electrolyte. There is also no evidence showing that the negatively charged thiols adsorbed on the negatively charged silica surface under any of the conditions examined.

**Measurement of Thiol Adsorption.** In this work, the adsorption of the charged thiol (0.5 mM $HSC_{10}COO^-$) on a gold substrate from its aqueous solution at pH 10.2 was monitored in situ as a function of adsorption time. The reason for choosing the concentration of the thiol at 0.5 mM is twofold. First, this concentration falls in the typical concentration range of a thiol solution (0.1−5.0 mM) for preparing a SAM surface. Second, this relatively high bulk concentration provides a sufficient supply of thiol for adsorption, so that significant depletion of thiol from the bulk does not occur during adsorption. Thus, the adsorption kinetics can be studied without complications from solution diffusion processes. On the other hand, as shown in a previous study,[11] the surface-confined carboxylic acid groups have a surface p$K_a$ of 7.7 and are fully dissociated near pH 10.0. Therefore, the selection of a solution pH of 10.2 in this study ensures that mercaptoundecanoic acids both in the solution and adsorbed on gold are completely deprotonated. This is important because any adsorbed negatively charged thiols can be registered in the force curves in this way, while those remaining in solution just function as electrolyte.

The interaction between the silica probe and the clean gold surface in aqueous solutions containing the charged thiols was repulsive and showed a strong time dependence. In Figure 2, we show typical force−separation curves obtained in 0.5 mM $HSC_{10}COO^-$ aqueous solution at several selected adsorption times, with the force scaled to the probe radius ($R = 8.0$ $\mu$m). As reported in earlier studies,[11,19] the interaction between silica and clean gold surfaces in deionized water at neutral pH exhibited an attractive interaction. However, with the addition of the negatively charged thiols into the solution, this interaction became repulsive, presumably due to the adsorption of the charged thiol on gold. For example, the force curve obtained at an adsorption time of 20 s (the shortest time that a stable force curve can be collected) showed an electrostatic repulsive force between the negative silica probe and the gold substrate, indicating that the gold substrate was negatively charged by the adsorption of thiols with terminal carboxylate ions. The electrostatic repulsive force increased with an increase in adsorption time, signaling negative charge building up on the substrate as more and more thiols adsorbed on gold. After 2−3 h of adsorption time, the electrostatic repulsive force no longer increased with an increase of adsorption time, showing that the surface charge remained constant after this time. To check if this constant surface charge represents the surface charge of a fully covered SAM/Au substrate, an alternative method was employed to prepare the SAM-covered gold substrate. A freshly prepared clean gold surface was immersed in a 5 mM mercaptoundecanoic acid ethanolic solution for 24 h. With the self-assembled monolayers of mercaptoundecanoic acid on gold, the formation of hydrogen bonds between terminal carboxylic acid groups is believed to facilitate compact monolayer formation.[26] This SAM-covered gold surface can serve as the model of a fully covered SAM/Au substrate. The force curves obtained with this compact SAM surface under the same solution conditions were identical to those collected after 2−3 h of adsorption time, suggesting that the thiol adsorption process reached the saturation stage after 2−3 h.

In a separate experiment, the reversibility of the thiol adsorption process was examined at several adsorption times (5, 30, and 120 min). This was accomplished by interrupting the adsorption process at different stages and replacing the thiol-containing solution by a 0.5 mM NaCl solution (pH 10.2). The resulting force curves remained unchanged up to 3 h. If significant thiol desorption did occur, then a decrease in the electrostatic repulsive force should be detected. The unchanged force curves obtained in NaCl solutions suggest that the thiol desorption is negligible and the adsorption process is irreversible.

The nature of the diffuse double layer can be exploited to explain the obtained electrostatic repulsive force between the negative silica tip and the thiol-adsorbed gold substrate (Figure 2). The diffuse double layer near the gold substrate is probed by the spherical silica tip as it moves through the double layer, which consists of counterions that compensate the charge residing at the gold/solution interface. For example, at an adsorption time of 30 min, the net surface charge of the gold substrate becomes negative, and a diffuse double layer with a net positive charge forms near the gold substrate. This positively charged diffuse double layer consists of a higher local concentration of $Na^+$ and $H^+$ and a lower local concentration of $HSC_{10}COO^-$ and $OH^-$. Therefore, as the negatively charged silica probe (with its own positively charged diffuse double layer) penetrates this double layer near the gold substrate, the overlap of the two positively charged double layers results in an electrostatic repulsive force.

The surface electrostatic potentials ($\psi$) of the thiol-adsorbed gold substrate can be calculated from the force data. In this work, the method of Hillier et al.[19] was used to calculate the electrical double-layer interaction between silica and gold surfaces. With knowledge of the silica probe surface potential, the surface electrostatic potentials of the thiol-covered gold substrate were obtained by theoretical fits of the force data to solutions of the complete nonlinear Poisson−Boltzmann equation. Figure 3 shows the results of theoretical curves fit to experimental force data at several selected adsorption times. All calculations include both electrostatic and van der Waals interactions, with $A_H = 1.1 \times 10^{-19}$ J and $\kappa^{-1} = 11.5$ nm. The observed Debye length corresponds closely to that expected with

---

[26] Crooks, R. M.; Sun, L.; Xu, C.; Hill, S. L.; Ricco, A. *J. Spectrosc.* **1993**, *8*, 28.

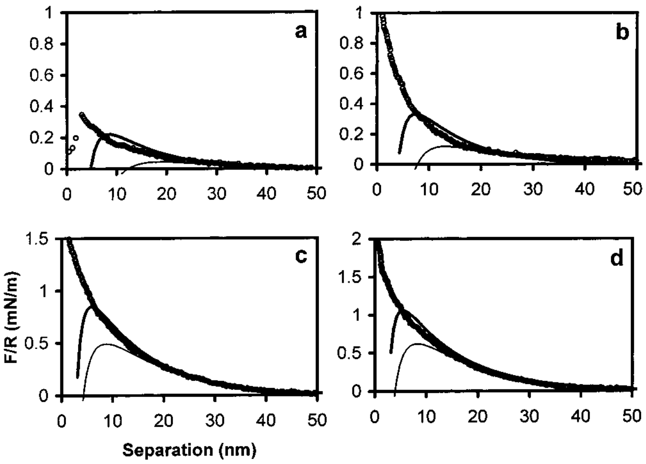

**Figure 3.** Measured (circles) and theoretical (solid lines) force between a silica probe and the thiol-adsorbed gold substrate at constant charge (thick line) and constant potential (thin line) at adsorption times of (a) 0.33, (b) 2.5, (c) 30, and (d) 180 min. In each fit, $A_H = 1.1 \times 10^{-19}$ J and $\kappa^{-1} = 11.5$ nm. The silica probe surface potential $\psi_p = -55$ mV. The best-fit parameters for all force curves are given in Table 1.

the free ion concentration of 0.7 mM in the solution, i.e., 0.5 mM $HSC_{10}COO^-$ and 0.2 mM $OH^-$ (pH 10.2). The boundary condition assuming a constant surface charge (thick line) provided a better fit than that assuming a constant potential (thin line), as found in previous work.[18e,19] However, both conditions deviate severely from the experimental data at separations of less than 10 nm. Several factors that are probably responsible for the deviation are the inaccuracy of the $A_H$ value, the ill-defined location for the plane of surface charge due to roughness of the silica probe and gold substrate, and the exclusion of the solvent repulsion term from the theoretical curves.[11,19] In Figure 3a, showing the force data obtained at an adsorption time of 20 s, the best fit gives a surface electrostatic potential of the gold substrate of $\psi_s = -18$ mV, with the known silica probe surface potential of $\psi_p = -55$ mV. The best-fit parameters for other force data are given in Table 1. The surface charge ($\sigma$) in Table 1 was calculated from the corresponding surface potential.[27] Recent work on electrochemically addressable monolayers[28] has shown that the surface charge measured by this AFM technique represents only a small fraction (~3%) of the total surface charge, which comprises that of a packed monolayer on the surface (26 $\mu$C/cm$^2$). This can be ascribed to charge neutralization of the monolayer by tight counterion binding, as found with polyelectrolytes.[29] Although one would expect the extent of this binding to be a function of surface coverage, measurements suggest that the fraction of tight ion binding is not a strong function of total surface charge at higher coverages. The deviations shown in Figures 4 and 5 may be caused by this effect. Given that the measured surface charge is directly related to the amount of the charged thiol adsorbed on the gold substrate, the surface coverage ($\theta$) at any adsorption time can be calculated with the knowledge of the surface charge of the fully covered SAM/Au substrate ($\sigma_m$). The results are also given in Table 1. Figure 4 shows a representative plot of $\theta$ vs time (solid circles) during adsorption of $HSC_{10}COO^-$ from 0.5 mM aqueous solution.

**Table 1. Force Data Analysis Results of the Thiol-Adsorbed Gold Substrate as a Function of Adsorption Time for 0.5 and 0.05 mM Concentrations of $HSC_{10}OO^-$ [a]**

| adsorption | surface potential, $\psi_s$ (mV) | | surface charge, $\sigma$ ($\mu$C/cm$^2$) | | surface coverage, $\theta^b$ | |
|---|---|---|---|---|---|---|
| time (min) | 0.5 | 0.05 | 0.5 | 0.05 | 0.5 | 0.05 |
| 0 | 0 | 0 | 0 | 0 | 0 | 0 |
| 0.33 | −18 | −9 | −0.11 | −0.05 | 0.19 | 0.09 |
| 1 | −24 | −13 | −0.15 | −0.08 | 0.26 | 0.14 |
| 2.5 | −27 | −13 | −0.17 | −0.08 | 0.29 | 0.14 |
| 5 | −36 | −20 | −0.24 | −0.12 | 0.41 | 0.21 |
| 10 | −42 | −30 | −0.28 | −0.19 | 0.48 | 0.33 |
| 15 | −49 | −35 | −0.34 | −0.23 | 0.59 | 0.39 |
| 20 | −53 | −39 | −0.38 | −0.26 | 0.66 | 0.45 |
| 30 | −59 | −45 | −0.44 | −0.31 | 0.76 | 0.53 |
| 45 | −64 | −52 | −0.50 | −0.37 | 0.86 | 0.64 |
| 60 | −66 | −56 | −0.52 | −0.41 | 0.90 | 0.71 |
| 90 | −67 | −61 | −0.53 | −0.46 | 0.91 | 0.80 |
| 120 | −69 | −64 | −0.55 | −0.49 | 0.95 | 0.85 |
| 150 | −70 | −66 | −0.57 | −0.52 | 0.98 | 0.89 |
| 180 | −72 | −68 | −0.59 | −0.54 | 1.02 | 0.94 |
| 210 | −71 | −70 | −0.58 | −0.57 | 1.00 | 0.98 |
| 240 | −72 | −71 | −0.59 | −0.58 | 1.02 | 1.00 |
| 300 | −72 | −71 | −0.59 | −0.58 | 1.02 | 1.00 |
| 360 | −71 | −70 | −0.58 | −0.57 | 1.00 | 0.98 |
| 1440 | −71 | −71 | −0.58 | −0.58 | 1.00 | 1.00 |

[a] Force data were obtained between a silica probe and gold substrate in a 0.5 mM $HSC_{10}COO^-$ and a 0.05 mM $HSC_{10}COO^-$ and 0.45 mM NaCl aqueous solution at pH 10.2 as a function of adsorption time. The silica probe surface potential $\psi_p = -55$ mV. All calculations include both electrostatic and van der Waals interactions with $A_H = 1.1 \times 10^{-19}$ J and $\kappa^{-1} = 11.5$ nm. [b] Surface coverage was calculated from $\theta = \sigma/\sigma_m$, where $\sigma_m$ is the measured surface charge of the fully covered gold substrate obtained by immersing a clean gold surface into 5 mM $HSC_{10}COOH$ ethanolic solution for 24 h.

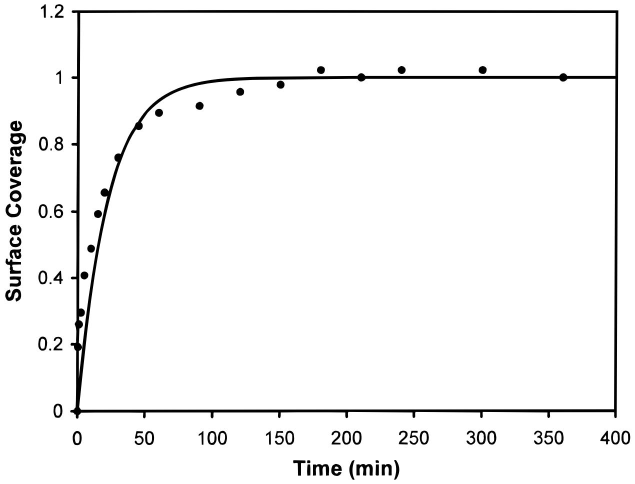

**Figure 4.** Representative plot of surface coverage vs time (solid circles) during adsorption of 0.5 mM $HSC_{10}COO^-$ from its aqueous solution of pH 10.2. The theoretical fit of the Langmuir rate law is represented by the solid line. The best theoretical fit gives an adsorption rate constant of 0.045 ± 0.005 min$^{-1}$.

To check the concentration dependence of the SAM formation process, similar force measurements between a silica probe and a gold substrate were conducted in an aqueous solution of 0.05 mM $HSC_{10}COO^-$ and 0.45 mM NaCl at pH 10.2. For comparison, NaCl was added to the solution to maintain the same ionic strength. The surface potential and charge of the charged thiol-adsorbed gold substrate were calculated from the force data as described

---

(27) (a) The surface charge ($\sigma$) in Table 1 is calculated from the relationship[27b] $\sigma = \epsilon_0\epsilon_s\kappa(2kT/e)\sinh(e\psi/2kT)$, where $\kappa$ is the reciprocal Debye length of the electrolyte solution with a dielectric constant, $\epsilon_s$, taken to be 78.49 and assumed to be independent of surface charge change, and $\epsilon_0$ is the permittivity of free space. (b) Bard, A. J.; Faulkner, L. R. *Electrochemical Methods*; J. Wiley: New York, 1980.

(28) Hu, K.; Chai, Z.; Whitesell, J. K.; Bard, A. J., manuscript in preparation.

(29) Fendler, J. H. *Membrane Mimetic Chemistry*; Wiley: New York, 1982; pp 214−220.

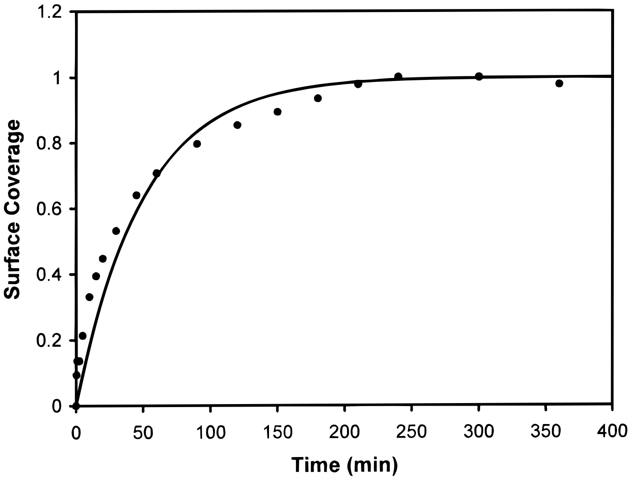

**Figure 5.** Representative plot of surface coverage vs time (solid circles) during adsorption from 0.05 mM $HSC_{10}COO^-$ and 0.45 mM NaCl aqueous solution of pH 10.2. The theoretical fit of the Langmuir rate law is represented by the solid line. The best theoretical fit gives an adsorption rate constant of $0.020 \pm 0.003$ $min^{-1}$.

earlier, and the results are also given in Table 1. A typical plot of $\theta$ vs time (solid circles) during adsorption of $HSC_{10}COO^-$ from its 0.05 mM aqueous solution is shown in Figure 5. Compared to the results shown in Figure 4, it is clear that the SAM formation process is dependent on thiol concentration, indicating that the solution diffusion processes begin to play their role in the SAM formation process at lower thiol concentrations, where significant depletion of thiol from the bulk occurs during adsorption. This is in line with previous work reported by Karpovich and Blanchard,[14] who monitored the thiol concentration dependence of QCM frequency change for 1-octadecanethiol in *n*-hexane.

**Rate Constant Deterimination.** To assess the thiol adsorption behavior, the Langmuir rate law was employed to fit the adsorption curve obtained here. Typically, if an adsorption process follows this rate law, then the rate of the surface adsorption is governed by the Langmuir isotherm, which is given by[14]

$$d\theta/dt = k_a(1 - \theta)C - k_d\theta \tag{1}$$

where $\theta$ is the fraction of surface covered, $(1 - \theta)$ is the fraction of surface unoccupied, $C$ is the bulk thiol concentration, and $k_a$ and $k_d$ are the intrinsic rate constants for adsorption and desorption, respectively. Integration of eq 1 gives the time-dependent surface coverage.

$$\theta(t) = [k_aC/(k_aC + k_d)][1 - \exp(-(k_aC + k_d))] \tag{2}$$

As stated earlier, the thiol desorption process is negligible, i.e., $k_d \ll k_a$. With the substitution of $k_{obs} = k_aC + k_d$, the simplified eq 2 gives

$$\theta(t) = 1 - \exp(-k_{obs}t) \tag{3}$$

Thus, with an assumed $k_{obs}$ value, the surface coverage at any given time can be calculated. Nevertheless, one should realize that the application of the Langmuir rate law to the SAM formation process is a simplification, especially at lower concentrations, where the solution diffusion processes can limit the rate of the adsorption process. The solid lines in Figures 4 and 5 represent the best fit to the experimental data with observed adsorption rate constants ($k_{obs}$) of $0.045 \pm 0.005$ and $0.020 \pm 0.003$ $min^{-1}$, respectively. Note that an increase in the rate of growth by a factor of 2.25 is observed with an increase in concentration by a factor of 10. The reasons for the dependence of the rate of growth on cubic concentration are not clear. For the adsorption from 0.5 mM $HSC_{10}COO^-$ aqueous solution (Figure 4), the characteristic time for the SAM formation, $k_{obs}{}^{-1} \approx 22$ min, is comparable with that found with QCMs by Shimazu et al.[12] (10−100 min) and by Pan et al.[15] (100 min) for alkanethiol adsorption on gold from ethanol solutions, but is much longer than that reported by Karpovich and Blanchard[14] (~10 s).

As shown in both Figures 4 and 5, although the adsorption can generally be described by a Langmuir rate law, as observed by Karpovich and Blanchard, examination of both figures indicates that an exponential fit does not match precisely with the experimental data. The adsorption process seems to be a fast process in early stages, followed by a slower process. The two-step process (a fast step followed by a slow step) was observed before by Bain et al.[4] and Pan et al.[15] using a QCM. In our system, there exists a fast step in early stages of the layer formation; i.e., for the adsorption from 0.5 mM $HSC_{10}COO^-$ aqueous solution, the surface coverage reaches 60% within the first 15 min and is followed by a slow process where full surface coverage is attained in about 2−3 h. Note that the experimental conditions in this work are different from those of the previous studies; i.e., we monitored the adsorption of a negatively charged thiol (rather than neutral alkanethiols) on gold from aqueous solution (rather than organic solvents). Due to the repulsive interaction between adsorbed charged thiols, the rate of the adsorption process in this work, especially the second step, is probably slower than that of the adsorption of alkanethiols, where the interchain hydrophobic interaction is favorable for the self-assembling process.

## Conclusion

An AFM was used to monitor in situ the adsorption process of a charged thiol ($HSC_{10}COO^-$) on gold from its aqueous solution. The diffuse double-layer interaction forces between a negative silica tip and the thiol-covered gold substrate were measured as a function of adsorption time. The surface charge and potential of the gold substrate were calculated from the force data with the knowledge of the silica probe surface potential. The fit of a Langmuir rate law to the surface coverage vs time data yielded overall adsorption rate constants. The self-assembly process was a two-step process, a fast step followed by a slower one.

**Acknowledgment.** The support of this research by grants from the National Renewable Energy Laboratory of the U.S. Department of Energy and the National Science Foundation (CHE-9508525) is gratefully acknowledged. The authors thank Professor Richard M. Crooks (Texas A & M University) for the sample of mercaptoundecanoic acid, Dr. Stephen W. Feldberg (Brookhaven National Laboratory) for helpful discussions, and Dr. Andrew C. Hillier (University of Virginia) for providing the computer program for the calculation of electrical double-layer forces. K.H. greatly appreciates support in the form of an ACS Division of Analytical Chemistry Fellowship sponsored by Procter & Gamble.

LA971363O